Chiral Symmetry and the Nucleon-Nucleon Interaction*

R. Machleidt†
Department of Physics, University of Idaho,
Moscow, ID 83843, U. S. A.

D. R. Entem‡
Grupo de Fisica Nuclear and IUFFyM, University of Salamanca,
E-37008 Salamanca, Spain

October 14, 2011

Abstract

We summarize the current status of our understanding of nuclear forces based upon chiral symmetry—an idea that was advocated by Gerry Brown already several decades ago.

1 Introduction

Forty years ago, Gerry Brown published the Comment "Isn't it Time to Calculate the Nucleon-Nucleon Force" [1], and more than 30 years ago, he wrote a book chapter entitled "Chiral Symmetry and the Nucleon-Nucleon Interaction"[2]. In fact, as early as 1968, he had published, together with two co-workers, a paper [3] on three-nucleon forces, where the consequences of chiral symmetry were fully exploited. Nevertheless, it should take a few more *decades* until the problem of the nucleon-nucleon (NN) interaction was really solved taking chiral symmetry consistently into account—and this fact proves the very advanced nature of Gerry's ideas concerning nuclear forces. It is the purpose of this contribution to summarize where we are today in our understanding of nuclear forces, based upon concepts that Gerry advocated already many decades ago.

But let's first recall more of the interesting history of the idea of chiral symmetry. The modern understanding is that this symmetry arises because the up and down quarks happen to have relatively small masses. However, chiral symmetry and its significance for low-energy hadron (pion) physics was discovered long before QCD. In 1960, based upon concepts proposed by Schwinger [4], Gell-Mann and Levy [5] developed the sigma model, which is a linear realization of chiral symmetry.[1] One major problem researchers had been struggling with in the 1950's was that the pion-nucleon scattering length came out two orders of magnitude too large when the (renormalizable) pseudo-scalar (γ_5) πN interaction was used. This unrealistic prediction was due to very large contributions from virtual anti-nucleon states (the so-called "pair terms" or "Z-graphs"). Similar problems occurred in the 2π-exchange contribution to the NN interaction. In the sigma model, the large pair terms are cancelled by processes involving the (fictitious) σ boson. In this way, the linear sigma model demonstrates how imposing chiral invariance fixes the problem with low-energy π-N scattering. However, the fictitious character of the σ particle as well as the reliance on the perfect cancelation

*Chapter 14 of: *From Nuclei to Stars—Festschrift in Honor of Gerald E. Brown*, edited by Sabine Lee (World Scientific, Singapore, 2011), p. 317-343.
†Electronic address: machleid@uidaho.edu
‡Electronic address: entem@usal.es
[1]For a pedagogical introduction into chiral symmetry and the sigma model, see [6].

of huge terms are uncomfortable features. In 1967, motivated by the current algebra approach to soft pion physics, Weinberg [7] worked out what has become known as the non-linear sigma model, which does not include a σ anymore and has pions and nucleons interact via pseudo-vector (derivative, $\gamma_5\gamma^\mu\partial_\mu$) coupling besides a new (non-linear) $\pi\pi NN$ term also involving a derivative ("Weinberg-Tomozawa term" [8, 9]). The derivative (equivalent to momentum) guarantees that the interaction vanishes when the momentum goes to zero providing a natural explanation for the weakness of the interaction by soft pions which does not rely on the cancellation of large terms. Following suggestions by Schwinger, Weinberg [10] developed, soon after, a general theory of non-linear realizations of chiral symmetry, which was further generalized in an elegant way by Callan, Coleman, Wess, and Zuimino [11].

However, ideas were needed for how to implement chiral symmetry consistently in the theory of pionic and nuclear interactions and how to deal with renormalization, since the derivative coupling is not renormalizable in the conventional sense. In his contribution to the 'Festschrift' in honor of Schwinger of 1979 [12, 13], Weinberg proposed to consider the most general possible Langrangian including all higher-derivative terms that are consistent with chiral symmetry (besides the other commonly assumed symmetry principles). For this theory to be manageable, one needs to assume some sort of perturbative expansion such that only a finite number of terms contribute at a given order. This expansion is provided by powers of small external momenta over the chiral symmetry breaking scale, $\Lambda_\chi \sim 1$ GeV. The higher-derivative terms supply the counterterms that make possible an order-by-order renormalization, which is the appropriate renormalization procedure for an effective field theory. Weinberg's suggestions were soon picked up by Gasser, Leutwyler, and associates who worked out, to one loop, the cases of $\pi\pi$ [14] and πN scattering [15] with great success.

But there was still the problem of the nuclear force which is more difficult, since nuclear interactions do not vanish in the chiral limit ($q \rightarrow 0$; $m_{u/d}, m_\pi \rightarrow 0$) and require a non-perturbative treatment because of the existence of nuclear bound states. In a series of papers published around 1990 [16, 17, 18], Weinberg picked up the nuclear force issue and suggested to calculate the NN potential perturbatively in the chiral expansion and then iterate it to all orders in a Schroedinger or Lippmann-Schwinger equation to obtain the nuclear amplitude. Here, the introduction of four-nucleon contact terms is crucial for renormalization.

Following the Weinberg proposal, pioneering work was performed by Ordóñez, Ray, and van Kolck [19, 20] who applied time-ordered perturbation theory to construct a NN potential up to next-to-next-to-leading order (NNLO). The results were encouraging and nuclear EFT quickly developed into one of the most popular branches of modern nuclear physics. The Munich group used covariant perturbation theory and dimensional regularization to calculated the perturbative NN amplitude without [21] and with $\Delta(1232)$-isobar degrees of freedom [22] at NNLO. Besides this, the Munich group worked out important loop contributions of higher order [23, 24, 25, 26, 27]. A relativistic approach was also taken by the Brazil group [28, 29]. The Bochum-Jülich group devised a method of unitarity transformations to eliminate the energy-dependence of time-ordered perturbation theory amplitudes and calculated the NN potentials up to NNLO [30, 31]. The Idaho group managed to construct a chiral NN potential at next-to-next-to-next-to-leading order (N^{3}LO) and showed that only at this order can one achieve the precision necessary for reliable few-nucleon and nuclear structure calculations [32, 33, 34, 35]. Progress extended beyond the NN interaction, as nuclear many-body forces based upon chiral perturbation theory were also developed [18, 36, 37, 38, 39].

During the past decade or so, chiral two-nucleon forces have been used in many microscopic calculations of nuclear reactions and structure [40, 41, 42, 43, 44, 45, 46, 47, 48, 49, 50, 51, 52, 53, 54, 55] and the combination of chiral two- and three-nucleon forces has been applied in few-nucleon reactions [37, 56, 57, 58, 59, 60, 61, 62, 63, 64], structure of light- and medium-mass nuclei [65, 66, 67, 68], and nuclear and neutron matter [69, 70]—with a great deal of success. The majority of nuclear structure calculations is nowadays based upon chiral forces.

This article is organized as follows. In Section 2, we sketch the essential ideas of an EFT for low-energy QCD. Section 3 provides an overview on nuclear forces derived from chiral EFT. The two-nucleon force is then discussed in detail in Section 4. Many-body forces are the subject of Section 5. Finally, Section 6 contains our conclusions.

2 Low-energy QCD and effective field theory

Quantum chromodynamics (QCD) is the theory of strong interactions. It deals with quarks, gluons and their interactions and is part of the Standard Model of Particle Physics. QCD is a non-Abelian gauge field theory with color $SU(3)$ the underlying gauge group. The non-Abelian nature of the theory has dramatic consequences. While the interaction between colored objects is weak at short distances or high momentum transfer ("asymptotic freedom"); it is strong at long distances ($\gtrsim 1$ fm) or low energies, leading to the confinement of quarks into colorless objects, the hadrons. Consequently, QCD allows for a perturbative analysis at large energies, whereas it is highly non-perturbative in the low-energy regime. Nuclear physics resides at low energies and the force between nucleons is a residual color interaction similar to the van der Waals force between neutral molecules. Therefore, in terms of quarks and gluons, the nuclear force is a very complicated problem that, nevertheless, can be attacked with brute computing power on a discretized, Euclidean space-time lattice (known as lattice QCD). Advanced lattice QCD calculations [71, 72] are under way and will yield improving results in the near future. However, since these calculations are very time-consuming and expensive, they can only be used to check a few representative key-issues. For everyday nuclear structure physics, a more efficient approach is needed.

The efficient approach is an effective field theory. For the development of an EFT, it is crucial to identify a separation of scales. In the hadron spectrum, a large gap between the masses of the pions and the masses of the vector mesons, like $\rho(770)$ and $\omega(782)$, can clearly be identified. Thus, it is natural to assume that the pion mass sets the soft scale, $Q \sim m_\pi$, and the rho mass the hard scale, $\Lambda_\chi \sim m_\rho$, also known as the chiral-symmetry breaking scale. This is suggestive of considering an expansion in terms of the soft scale over the hard scale, Q/Λ_χ. Concerning the relevant degrees of freedom, we noticed already that, for the ground state and the low-energy excitation spectrum of an atomic nucleus as well as for conventional nuclear reactions, quarks and gluons are ineffective degrees of freedom, while nucleons and pions are the appropriate ones. To make sure that this EFT is not just another phenomenology, it must have a firm link with QCD. The link is established by having the EFT observe all relevant symmetries of the underlying theory. This requirement is based upon a 'folk theorem' by Weinberg [12]:

> If one writes down the most general possible Lagrangian, including *all* terms consistent with assumed symmetry principles, and then calculates matrix elements with this Lagrangian to any given order of perturbation theory, the result will simply be the most general possible S-matrix consistent with analyticity, perturbative unitarity, cluster decomposition, and the assumed symmetry principles.

Since the up and down quark masses are very small, one may assume (approximate) chiral symmetry which, however, is broken in two ways. It is explicitly broken, because the the up and down quark masses are not exactly zero. Moreover, we are also faced with so-called spontaneous symmetry breaking.

A (continuous) symmetry is said to be *spontaneously broken* if a symmetry of the Lagrangian is not realized in the ground state of the system. There is evidence that the (approximate) chiral symmetry of the QCD Lagrangian is spontaneously broken—for dynamical reasons of nonperturbative origin which are not fully understood at this time. The most plausible evidence comes from the hadron spectrum. From chiral symmetry, one would naively expect the existence of degenerate hadron multiplets of opposite parity, i.e., for any hadron of positive parity one would expect a degenerate hadron state of negative parity and vice versa. However, these "parity doublets" are not observed in nature. For example, take the ρ-meson which is a vector meson of negative parity ($J^P = 1^-$) and mass 776 MeV. There does exist a 1^+ meson, the a_1, but it has a mass of 1230 MeV and, thus, cannot be perceived as degenerate with the ρ. On the other hand, the ρ meson comes in three charge states (equivalent to three isospin states), the $\rho^\pm$ and the ρ^0, with masses that differ by at most a few MeV. In summary, in the hadron spectrum, $SU(2)_V$ (isospin symmetry) is well observed, while axial symmetry is broken: $SU(2)_L \times SU(2)_R$ is broken down to $SU(2)_V$.

A spontaneously broken global symmetry implies the existence of (massless) Goldstone bosons [73, 74]. The Goldstone bosons are identified with the isospin triplet of the (pseudoscalar) pions, which explains why pions are so light. The pion masses are not exactly zero because the up and down quark masses are not

exactly zero either. Thus, pions are a truly remarkable species: they reflect spontaneous as well as explicit symmetry breaking. Goldstone bosons interact weakly at low energy. They are degenerate with the vacuum and, therefore, interactions between them must vanish at zero momentum and in the chiral limit ($m_\pi \to 0$).

The next step is to build the most general Lagrangian consistent with the (broken) symmetries discussed above. An elegant formalism for the construction of such Lagrangians was developed by Callan, Coleman, Wess, and Zumino (CCWZ) [11] who worked out the group-theoretical foundations of non-linear realizations of chiral symmetry. It is characteristic for these non-linear realizations that, whenever functions of the Goldstone bosons appear in the Langrangian, they are always accompanied with at least one space-time derivative.

As discussed, the relevant degrees of freedom are pions (Goldstone bosons) and nucleons. Since the interactions of Goldstone bosons must vanish at zero momentum transfer and in the chiral limit ($m_\pi \to 0$), the low-energy expansion of the Lagrangian is arranged in powers of derivatives and pion masses. The hard scale is the chiral-symmetry breaking scale, $\Lambda_\chi \approx 1$ GeV. Thus, the expansion is in terms of powers of Q/Λ_χ where Q is a (small) momentum or pion mass. This is chiral perturbation theory (ChPT).

The effective Lagrangian can formally be written as,

$$\mathcal{L}_{\text{eff}} = \mathcal{L}_{\pi\pi} + \mathcal{L}_{\pi N} + \mathcal{L}_{NN} + \ \dots\ , \tag{1}$$

where $\mathcal{L}_{\pi\pi}$ deals with the dynamics among pions, $\mathcal{L}_{\pi N}$ describes the interaction between pions and a nucleon, and $\mathcal{L}_{NN}$ provides contact interactions between two nucleons. The individual Lagrangians are organized as follows:

$$\mathcal{L}_{\pi\pi} = \mathcal{L}_{\pi\pi}^{(2)} + \mathcal{L}_{\pi\pi}^{(4)} + \dots, \tag{2}$$

$$\mathcal{L}_{\pi N} = \mathcal{L}_{\pi N}^{(1)} + \mathcal{L}_{\pi N}^{(2)} + \mathcal{L}_{\pi N}^{(3)} + \dots, \tag{3}$$

and

$$\mathcal{L}_{NN} = \mathcal{L}_{NN}^{(0)} + \mathcal{L}_{NN}^{(2)} + \mathcal{L}_{NN}^{(4)} + \dots, \tag{4}$$

where the superscript refers to the number of derivatives or pion mass insertions (chiral dimension) and the ellipsis stands for terms of higher dimensions. See Ref. [33] for a concise summary of the explicit expressions for these Lagrangians.

3 Nuclear forces from chiral EFT: Overview

3.1 Chiral perturbation theory and power counting

As discussed, effective field theories (EFTs) are defined in terms of effective Langrangians which are given by an infinite series of terms with increasing number of derivatives and/or nucleon fields, with the dependence of each term on the pion field prescribed by the rules of broken chiral symmetry. Applying this Lagrangian to a particular process, an unlimited number of Feynman graphs can be generated. Therefore, we need a scheme that makes the theory manageable and calculable. This scheme which tells us how to distinguish between large (important) and small (unimportant) contributions is chiral perturbation theory (ChPT), and determining the power ν of the expansion has become known as power counting.

Nuclear potentials are defined as sets of irreducible graphs up to a given order. The power ν of a few-nucleon diagram involving A nucleons is given in terms of naive dimensional analysis by:

$$\nu = -2 + 2A - 2C + 2L + \sum_i \Delta_i\,, \tag{5}$$

with

$$\Delta_i \equiv d_i + \frac{n_i}{2} - 2\,, \tag{6}$$

where C denotes the number of separately connected pieces and L the number of loops in the diagram; d_i is the number of derivatives or pion-mass insertions and n_i the number of nucleon fields (nucleon legs) involved

in vertex i; the sum runs over all vertices contained in the diagram under consideration. Note that $\Delta_i \geq 0$ for all interactions allowed by chiral symmetry. For an irreducible NN diagram ("two-nucleon force", $A = 2$, $C = 1$), Eq. (5) collapses to

$$\nu = 2L + \sum_i \Delta_i \,. \tag{7}$$

In summary, the chief point of the ChPT expansion is that, at a given order ν, there exists only a finite number of graphs. This is what makes the theory calculable. The expression $(Q/\Lambda_\chi)^{\nu+1}$ provides a rough estimate of the relative size of the contributions left out and, thus, of the accuracy at order ν. In this sense, the theory can be calculated to any desired accuracy and has predictive power.

3.2 The hierarchy of nuclear forces

Chiral perturbation theory and power counting imply that nuclear forces emerge as a hierarchy controlled by the power ν, Fig. 1.

In lowest order, better known as leading order (LO, $\nu = 0$), the NN amplitude is made up by two momentum-independent contact terms ($\sim Q^0$), represented by the four-nucleon-leg graph with a small-dot vertex shown in the first row of Fig. 1, and static one-pion exchange (1PE), second diagram in the first row of the figure. This is, of course, a rather crude approximation to the two-nucleon force (2NF), but accounts already for some important features. The 1PE provides the tensor force, necessary to describe the deuteron, and it explains NN scattering in peripheral partial waves of very high orbital angular momentum. At this order, the two contacts which contribute only in S-waves provide the short- and intermediate-range interaction which is somewhat crude.

In the next order, $\nu = 1$, all contributions vanish due to parity and time-reversal invariance.

Therefore, the next-to-leading order (NLO) is $\nu = 2$. Two-pion exchange (2PE) occurs for the first time ("leading 2PE") and, thus, the creation of a more sophisticated description of the intermediate-range interaction is starting here. Since the loop involved in each pion-diagram implies already $\nu = 2$ [cf. Eq. (7)], the vertices must have $\Delta_i = 0$. Therefore, at this order, only the lowest order πNN and $\pi\pi NN$ vertices are allowed which is why the leading 2PE is rather weak. Furthermore, there are seven contact terms of $\mathcal{O}(Q^2)$, shown by the four-nucleon-leg graph with a solid square, which contribute in S and P waves. The operator structure of these contacts include a spin-orbit term besides central, spin-spin, and tensor terms. Thus, essentially all spin-isospin structures necessary to describe the two-nucleon force phenomenologically have been generated at this order. The main deficiency at this stage of development is an insufficient intermediate-range attraction.

This problem is finally fixed at order three ($\nu = 3$), next-to-next-to-leading order (NNLO). The 2PE involves now the two-derivative $\pi\pi NN$ seagull vertices (proportional to the c_i LECs) denoted by a large solid dot in Fig. 1. These vertices represent correlated 2PE as well as intermediate $\Delta(1232)$-isobar contributions. It is well-known from the meson phenomenology of nuclear forces [75, 76] that these two contributions are crucial for a realistic and quantitative 2PE model. Consequently, the 2PE now assumes a realistic size and describes the intermediate-range attraction of the nuclear force about right. Moreover, first relativistic corrections come into play at this order. There are no new contacts.

The reason why we talk of a hierarchy of nuclear forces is that two- and many-nucleon forces are created on an equal footing and emerge in increasing number as we go to higher and higher orders. At NNLO, the first set of nonvanishing three-nucleon forces (3NF) occur [36, 37], cf. column '3N Force' of Fig. 1. In fact, at the previous order, NLO, irreducible 3N graphs appear already, however, it has been shown by Weinberg [18] and others [36, 77, 78] that these diagrams all cancel. Since nonvanishing 3NF contributions happen first at order $(Q/\Lambda_\chi)^3$, they are very weak as compared to 2NF which start at $(Q/\Lambda_\chi)^0$.

More 2PE is produced at $\nu = 4$, next-to-next-to-next-to-leading order (N^{3}LO), of which we show only a few symbolic diagrams in Fig. 1. Two-loop 2PE graphs show up for the first time and so does three-pion exchange (3PE) which necessarily involves two loops. 3PE was found to be negligible at this order [23, 24]. Most importantly, 15 new contact terms $\sim Q^4$ arise and are represented by the four-nucleon-leg graph with a solid diamond. They include a quadratic spin-orbit term and contribute up to D-waves. Mainly due to

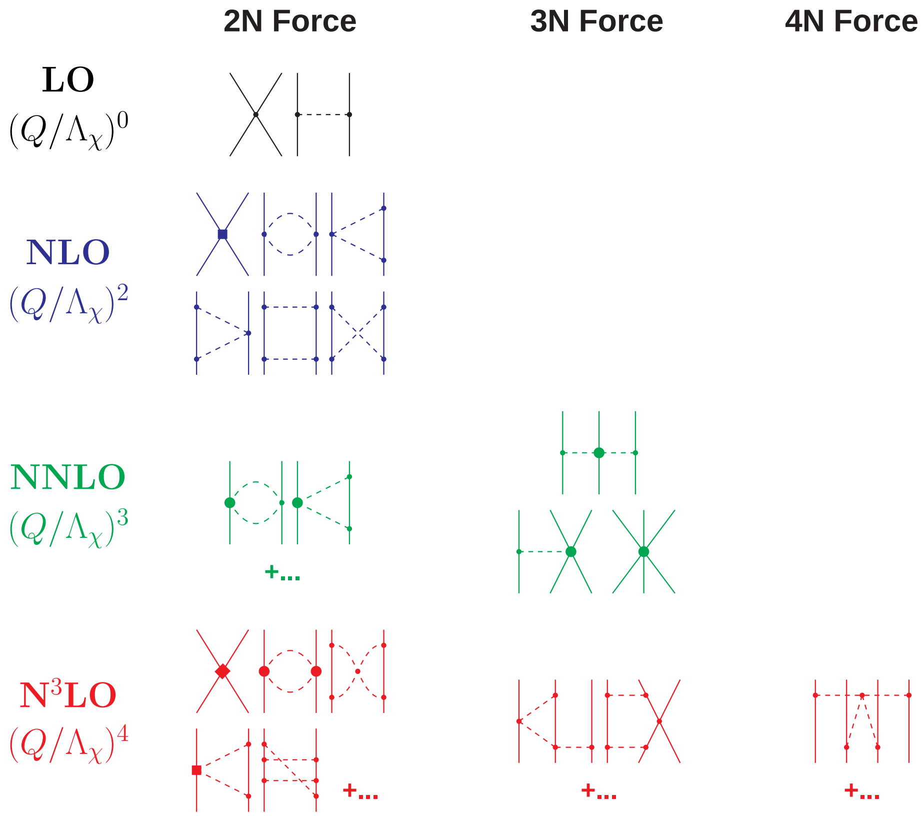

Figure 1: Hierarchy of nuclear forces in ChPT. Solid lines represent nucleons and dashed lines pions. Small dots, large solid dots, solid squares, and solid diamonds denote vertices of index $\Delta = 0$, 1, 2, and 4, respectively. Further explanations are given in the text.

the increased number of contact terms, a quantitative description of the two-nucleon interaction up to about 300 MeV lab. energy is possible, at N^{3}LO (for details, see below). Besides further 3NF, four-nucleon forces (4NF) start at this order. Since the leading order 4NF come into existence one order higher than the leading 3NF, 4NF are weaker than 3NF. Thus, ChPT provides a straightforward explanation for the empirically known fact that 2NF $\gg$ 3NF $\gg$ 4NF ....

4 The nucleon-nucleon interaction

4.1 Definition of the chiral NN potential

The previous section has provided us with an overview. In this section, we will now discuss the NN interaction in more detail. In terms of naive dimensional analysis or "Weinberg counting", the various orders of the irreducible graphs which define the chiral NN potential are given by:

$$V_{\rm LO} = V_{\rm ct}^{(0)} + V_{1\pi}^{(0)} \tag{8}$$

$$V_{\rm NLO} = V_{\rm LO} + V_{\rm ct}^{(2)} + V_{1\pi}^{(2)} + V_{2\pi}^{(2)} \tag{9}$$

$$V_{\rm NNLO} = V_{\rm NLO} + V_{1\pi}^{(3)} + V_{2\pi}^{(3)} \tag{10}$$

$$V_{\rm N^3LO} = V_{\rm NNLO} + V_{\rm ct}^{(4)} + V_{1\pi}^{(4)} + V_{2\pi}^{(4)} + V_{3\pi}^{(4)} \tag{11}$$

where the superscript denotes the order ν of the low-momentum expansion. LO stands for leading order, NLO for next-to-leading order, etc.. Contact potentials carry the subscript "ct" and pion-exchange potentials can be identified by an obvious subscript.

The one-pion exchange (1PE) potential reads

$$V_{1\pi}(\vec{p}\,',\vec{p}) = -\frac{g_A^2}{4f_\pi^2}\,\boldsymbol{\tau}_1\cdot\boldsymbol{\tau}_2\,\frac{\vec{\sigma}_1\cdot\vec{q}\,\vec{\sigma}_2\cdot\vec{q}}{q^2+m_\pi^2}\,, \tag{12}$$

where $\vec{p}\,'$ and $\vec{p}$ designate the final and initial nucleon momenta in the center-of-mass system and $\vec{q}\equiv\vec{p}\,'-\vec{p}$ is the momentum transfer; $\vec{\sigma}_{1,2}$ and $\boldsymbol{\tau}_{1,2}$ are the spin and isospin operators of nucleon 1 and 2; g_A, f_π, and m_π denote axial-vector coupling constant, the pion decay constant, and the pion mass, respectively. Since higher order corrections contribute only to mass and coupling constant renormalizations and since, on shell, there are no relativistic corrections, the on-shell 1PE has the form Eq. (12) up to all orders.

Multi-pion exchange, which starts at NLO and continues through all higher orders, involves divergent loop integrals that need to be regularized. An elegant way to do this is dimensional regularization which (besides the main nonpolynomial result) typically generates polynomial terms with coefficients that are, in part, infinite or scale dependent [21]. One purpose of the contacts is to absorb all infinities and scale dependencies and make sure that the final result is finite and scale independent. This is the renormalization of the perturbatively calculated NN amplitude (which, by definition, is the "NN potential"). It is very similar to what is done in the ChPT calculations of $\pi\pi$ and πN scattering, namely, a renormalization order by order, which is the method of choice for any EFT. Thus, up to this point, the calculation fully meets the standards of an EFT and there are no problems. The perturbative NN amplitude can be used to make model independent predictions for peripheral partial waves [21, 22, 33]. A concise summary of the explicit expressions for the 2π exchange contributions up to order N^{3}LO can be found in Ref. [33].

4.2 Regularization and renormalization

For calculations of the structure of nuclear few and many-body systems, the lower partial waves are the most important ones. The fact that in S waves we have large scattering lengths and shallow (quasi) bound states indicates that these waves need to be treated nonperturbatively. Following Weinberg's prescription [16], this is accomplished by inserting the potential V into the Lippmann-Schwinger (LS) equation:

$$T(\vec{p}\,',\vec{p}) = V(\vec{p}\,',\vec{p}) + \int d^3p''\,V(\vec{p}\,',\vec{p}\,'')\,\frac{M_N}{p^2-p''^2+i\epsilon}\,T(\vec{p}\,'',\vec{p})\,, \tag{13}$$

where M_N denotes the nucleon mass.

In general, the integral in the LS equation is divergent and needs to be regularized. One way to do this is by multiplying V with a regulator function

$$V(\vec{p}\,',\vec{p}) \longmapsto V(\vec{p}\,',\vec{p})\,\boldsymbol{e}^{-(p'/\Lambda)^{2n}}\;\boldsymbol{e}^{-(p/\Lambda)^{2n}}\,. \tag{14}$$

Typical choices for the cutoff parameter Λ that appears in the regulator are $\Lambda\approx 0.5$ GeV $\ll \Lambda_\chi \approx 1$ GeV.

It is pretty obvious that results for the T-matrix may depend sensitively on the regulator and its cutoff parameter. This is acceptable if one wishes to build models. For example, the meson models of the past [79, 75] always depended sensitively on the choices for the cutoff parameters which, in fact, were important for the fit of the NN data. However, the EFT approach wishes to be fundamental in nature and not just another model.

In field theories, divergent integrals are not uncommon and methods have been developed for how to deal with them. One regulates the integrals and then removes the dependence on the regularization parameters (scales, cutoffs) by renormalization. In the end, the theory and its predictions do not depend on cutoffs or renormalization scales.

So-called renormalizable quantum field theories, like QED, have essentially one set of prescriptions that takes care of renormalization through all orders. In contrast, EFTs are renormalized order by order.

As discussed, the renormalization of *perturbative* EFT calculations is not a problem. *The problem is nonperturbative renormalization.* This problem typically occurs in *nuclear* EFT because nuclear physics is characterized by bound states which are nonperturbative in nature. EFT power counting may be different for nonperturbative processes as compared to perturbative ones. Such difference may be caused by the infrared enhancement of the reducible diagrams generated in the LS equation.

Weinberg's implicit assumption [16, 13] was that the counterterms introduced to renormalize the perturbatively calculated potential, based upon naive dimensional analysis ("Weinberg counting"), are also sufficient to renormalize the nonperturbative resummation of the potential in the LS equation. In 1996, Kaplan, Savage, and Wise (KSW) [80] pointed out that there are problems with the Weinberg scheme if the LS equation is renormalized by minimally-subtracted dimensional regularization. This criticism resulted in a flurry of publications on the renormalization of the nonperturbative NN problem. See Ref. [81] for a thorough discussion, the bottom line of which is:

Crucial for an EFT are regulator independence (within the range of validity of the EFT) and a power counting scheme that allows for order-by-order improvement with decreasing truncation error. The purpose of renormalization is to achieve this regulator independence while maintaining a functional power counting scheme. After the comprehensive tries and errors of the past, it appears that there are two renormalization schemes which have the potential to achieve the above goals and, therefore, should be investigated systematically in the near future.

In *scheme one*, the LO calculation is conducted nonperturbatively (with $\Lambda \to \infty$ as in [82]) and subleading orders are added perturbatively in distorted wave Born approximation. Valderrama has started this in S waves [83], but results in higher partial waves are needed to fully assess this approach. Even though at this early stage any judgement is speculative, we take the liberty to predict that this approach will be only of limited success and utility—for the following reasons. First, it will probably require about twice as many counterterms as Weinberg counting and, therefore, will have less predictive power. Second, this scheme may converge badly, because the largest portion of the nuclear force, namely, the intermediate-range attraction appears at NNLO. Third, as discussed in [84], this force may be problematic (and, therefore, impractical) in applications in nuclear few- and many-body systems, because of a pathologically strong tensor force that will cause bad convergence of energy and wave functions. Finally, in the work that has been conducted so far within this scheme by Valderrama, it is found that only rather soft cutoffs can be used.

The latter point (namely, soft cutoffs) suggests that one may then as well conduct the calculation nonperturbatively at all orders (up to N^{3}LO) using Weinberg counting, which is no problem with soft cutoffs. This is *scheme two* that we propose to investigate systematically. In the spirit of Lepage [85], the cutoff independence should be examined for cutoffs below the hard scale and not beyond. Ranges of cutoff independence within the theoretical error are to be identified using 'Lepage plots'. A very systematic investigation of this kind does not exist at this time and is therefore needed. However, there is comprehensive circumstantial evidence from the numerous chiral NN potentials constructed over the past decade [20, 31, 33, 34, 35, 86] indicating that this investigation will most likely be a success (cf. also Fig. 2, below). The potentials discussed in the following section are all based upon Weinberg counting.

4.3 Constructing quantitative chiral NN potentials

4.3.1 What order?

As discussed, the NN potential can be calculated up to various orders, cf. Eqs. (8)-(11), and the accuracy increases as the order increases. That triggers the obvious question: To what order do we have to go for an accuracy that we would perceive as necessary and sufficient for, e. g., reliable microscopic nuclear structure calculations?

To answer this question, we show in Table 1 the χ^2/datum for the fit of the world np data below 290 MeV for families of np potentials at NLO and NNLO constructed by the Juelich group [89]. The NLO potentials produce the very large χ^2/datum between 67 and 105, and the NNLO are between 12 and 27. The rate of improvement from one order to the other is very encouraging, but the quality of the reproduction of the np data at NLO and NNLO is obviously insufficient for reliable predictions.

Table 1: Columns three and four show the χ^2/datum for the reproduction of the 1999 *np* database [87] (subdivided into energy intervals) by families of *np* potentials at NLO and NNLO constructed by the Juelich group [89]. The χ^2/datum is stated in terms of ranges which result from a variation of the cutoff parameters used in the regulator functions. The values of these cutoff parameters in units of MeV are given in parentheses. $T_{\rm lab}$ denotes the kinetic energy of the incident neutron in the laboratory system.

$T_{\rm lab}$ bin (MeV)	# of *np* data	— *Juelich np potentials* — NLO (550/700–400/500)	NNLO (600/700–450/500)
0–100	1058	4–5	1.4–1.9
100–190	501	77–121	12–32
190–290	843	140–220	25–69
0–290	2402	67–105	12–27

Based upon these facts, it has been pointed out in 2002 by Entem and Machleidt [32, 33] that one has to proceed to N^{3}LO. Consequently, the first N^{3}LO potential was published in 2003 [34].

At N^{3}LO, there are a total of 24 contact terms (24 parameters) which contribute to the partial waves with $L \leq 2$. These 24 LECs are essentially free constants which parametrize the short-ranged phenomenological part of the interaction. In Table 2, column 'Q^4/N^{3}LO', we show how these terms are distributed over the partial waves. Most important for the improved reproduction of the NN phase shifts (and NN observables) at N^{3}LO is the fact that contacts appear for the first time in D-waves. D-waves are not truely peripheral and, therefore, 1PE plus 2PE alone do not describe them well. The D-wave contacts provide the necessary short-range corrections to get the D-phases right. Besides this, at N^{3}LO, another contact is added to each P-wave, which leads to substantial improvements, particularly, in $^3P_0$ and $^3P_1$ above 100 MeV.

In Table 2, we also show the number of parameters used in the Nijmegen partial wave analysis (PWA93) [90] and in the high-precision CD-Bonn potential [88]. The table reveals that, for S and P waves, the number of parameters used in high-precision phenomenology and in EFT at N^{3}LO are about the same. **Thus, the EFT approach provides retroactively a justification for the phenomenology used in the 1990's to obtain high-precision fits.**

At NLO and NNLO, the number of contact parameters is substantially smaller than for PWA93 and CD-Bonn, which explains why these orders are insufficient for a quantitative potential. The 24 parameters of N^{3}LO are close to the 30+ used in PWA93 and high precision potentials. Consequently (see following sections for details), at N^{3}LO, a fit of the NN data is possible that is of about the same quality as the one by the high-precision NN potentials [91, 92, 93, 88]. Thus, one may perceive N^{3}LO as the order of ChPT that is necessary and sufficient for a reliable NN potential.

4.3.2 A quantitative NN potential at N^{3}LO

We choose the Idaho N^{3}LO potential [34] as example. Note that for an accurate fit of the low-energy *pp* and *np* data, charge-dependence is important. We include charge-dependence up to next-to-leading order of the isospin-violation scheme (NLØ, in the notation of Ref. [94]). Thus, we include the pion mass difference in 1PE and the Coulomb potential in *pp* scattering, which takes care of the LØ contributions. At order NLØ we have pion mass difference in the NLO part of TPE, $\pi\gamma$ exchange [95], and two charge-dependent contact interactions of order Q^0 which make possible an accurate fit of the three different $^1S_0$ scattering lengths, a_{pp}, a_{nn}, and a_{np}.

For the cutoff parameter Λ of the regulator Eq. (14), we choose initially 500 MeV. Within a certain reasonable range, results should not depend sensitively on Λ (cf. discussion in Section 4.2). Therefore, we have also made a second fit for $\Lambda = 600$ MeV.

The fitting procedure starts with the peripheral partial waves because they involve fewer and more

Table 2: Number of parameters needed for fitting the np data in phase-shift analysis and by a high-precision NN potential *versus* the total number of NN contact terms of EFT based potentials to different orders.

	Nijmegen partial-wave analysis [90]	CD-Bonn high-precision potential [88]	— *Contact Potentials* — Q^0 LO	Q^2 NLO/NNLO	Q^4 N^{3}LO
$^1S_0$	3	4	1	2	4
$^3S_1$	3	4	1	2	4
$^3S_1$-$^3D_1$	2	2	0	1	3
$^1P_1$	3	3	0	1	2
$^3P_0$	3	2	0	1	2
$^3P_1$	2	2	0	1	2
$^3P_2$	3	3	0	1	2
$^3P_2$-$^3F_2$	2	1	0	0	1
$^1D_2$	2	3	0	0	1
$^3D_1$	2	1	0	0	1
$^3D_2$	2	2	0	0	1
$^3D_3$	1	2	0	0	1
$^3D_3$-$^3G_3$	1	0	0	0	0
$^1F_3$	1	1	0	0	0
$^3F_2$	1	2	0	0	0
$^3F_3$	1	2	0	0	0
$^3F_4$	2	1	0	0	0
$^3F_4$-$^3H_4$	0	0	0	0	0
$^1G_4$	1	0	0	0	0
$^3G_3$	0	1	0	0	0
$^3G_4$	0	1	0	0	0
$^3G_5$	0	1	0	0	0
Total	35	38	2	9	24

fundamental parameters. Partial waves with $L \geq 3$ are exclusively determined by 1PE and 2PE because the N^{3}LO contacts contribute to $L \leq 2$ only. 1PE and 2PE at N^{3}LO depend on the axial-vector coupling constant, g_A (we use $g_A = 1.29$), the pion decay constant, $f_\pi = 92.4$ MeV, and eight low-energy constants (LECs) that appear in the dimension-two and dimension-three πN Lagrangians. The LECs are listed in Table 3, where column 'NN pot.' shows the values used for the present N^{3}LO potential. In the fitting process, we varied three of them, namely, c_2, c_3, and c_4. We found that the other LECs are not very effective in the NN system and, therefore, we left them at their central values as determined in πN analysis. The most influential constant is c_3, which—in terms of magnitude—has to be chosen on the low side (slightly more than one standard deviation below its πN determination), otherwise there is too much central attraction. Concerning c_4, our choice $c_4 = 5.4$ GeV^{-1} lowers the $^3F_2$ phase shift (and slightly the $^1F_3$) bringing it into closer agreement with the phase shift analysis—as compared to using the πN value $c_4 = 3.4$ GeV^{-1}. The other F waves and the higher partial waves are essentially unaffected by this variation of c_4. Finally, the change of c_2 from its πN value of 3.28 GeV^{-1} to 2.80 GeV^{-1} (our choice) brings about some subtle improvements of the fit, but it is not essential. Overall, the fit of all $J \geq 3$ waves is very good.

We turn now to the lower partial waves. Here, the most important fit parameters are the ones associated with the 24 contact terms that contribute to the partial waves with $L \leq 2$. In addition, we have two charge-dependent contacts which are used to fit the three different $^1S_0$ scattering lengths, a_{pp}, a_{nn}, and a_{np}.

In the optimization procedure, we fit first phase shifts, and then we refine the fit by minimizing the χ^2

Table 3: Low-energy constants applied in the N^{3}LO NN potential (column 'NN pot.'). The c_i belong to the dimension-two πN Lagrangian and are in units of GeV^{-1}, while the $\bar{d}_i$ are associated with the dimension-three Lagrangian and are in units of GeV^{-2}. The column 'πN analysis' shows values determined from πN data.

	NN pot.	πN analysis
c_1	–0.81	-0.81 ± 0.15^a
c_2	2.80	3.28 ± 0.23^b
c_3	–3.20	-4.69 ± 1.34^a
c_4	5.40	3.40 ± 0.04^a
$\bar{d}_1 + \bar{d}_2$	3.06	3.06 ± 0.21^b
$\bar{d}_3$	–3.27	-3.27 ± 0.73^b
$\bar{d}_5$	0.45	0.45 ± 0.42^b
$\bar{d}_{14} - \bar{d}_{15}$	–5.65	-5.65 ± 0.41^b

[a]Table 1, Fit 1 of Ref. [96]. [b]Table 2, Fit 1 of Ref. [97].

Table 4: Columns three to five display the χ^2/datum for the reproduction of the 1999 ***np* database** [87] (subdivided into energy intervals) by various *np* potentials. For the chiral potentials, the χ^2/datum is stated in terms of ranges which result from a variation of the cutoff parameters used in the regulator functions. The values of these cutoff parameters in units of MeV are given in parentheses. $T_{\rm lab}$ denotes the kinetic energy of the incident nucleon in the laboratory system.

$T_{\rm lab}$ bin (MeV)	# of ***np*** data	*Idaho* N^{3}LO [34] (500–600)	*Juelich* N^{3}LO [86] (600/700–450/500)	Argonne V_{18} [92]
0–100	1058	1.0–1.1	1.0–1.1	0.95
100–190	501	1.1–1.2	1.3–1.8	1.10
190–290	843	1.2–1.4	2.8–20.0	1.11
0–290	2402	1.1–1.3	1.7–7.9	1.04

obtained from a direct comparison with the data. We start with *pp*, since the *pp* phase shifts and data are more accurate than the *np* ones. The *pp* fit fixes essentially the $I = 1$ potential. The $I = 1$ *np* potential is just the *pp* one modified by charge-dependence due to nucleon-mass difference, pion-mass splitting in 1PE, $\pi\gamma$ exchange, and omission of Coulomb. In addition to this, the non-derivative contact in the $^1S_0$ state is changed such as to reproduce the *np* scattering length. The *nn* potential is the *pp* one without Coulomb, using neutron masses, and fitting the *nn* scattering length in the $^1S_0$ state with the non-derivative contact.

The χ^2/datum for the fit of the *np* data below 290 MeV are shown in Table 4, and the corresponding ones for *pp* are given in Table 5. These tables reveal that at N^{3}LO a χ^2/datum comparable to the high-precision Argonne V_{18} [92] potential can, indeed, be achieved. The Idaho N^{3}LO potential [34] with $\Lambda = 500$ MeV produces a χ^2/datum = 1.1 for the world *np* data below 290 MeV which compares well with the χ^2/datum = 1.04 by the Argonne potential. In 2005, also the Juelich group produced several N^{3}LO NN potentials [86], the best of which fits the *np* data with a χ^2/datum = 1.7 and the worse with 7.9 (Table 4).

Turning to *pp*, the χ^2 for *pp* data are typically larger than for *np* because of the higher precision of *pp* data. Thus, the Argonne V_{18} produces a χ^2/datum = 1.4 for the world *pp* data below 290 MeV and the best Idaho N^{3}LO *pp* potential obtains 1.5. The fit by the best Juelich N^{3}LO *pp* potential results in a χ^2/datum = 2.9 and the worst produces 22.3.

Phase shifts of *np* scattering from two Idaho (solid and dashed lines) and two Juelich (dash-dotted and dotted lines) N^{3}LO *np* potentials are shown in Figs. 2. The phase shifts confirm what the corresponding χ^2

Table 5: Same as Table 4 but for ***pp***.

$T_{\rm lab}$ bin (MeV)	# of ***pp*** data	*Idaho* N^{3}LO [34] (500–600)	*Juelich* N^{3}LO [86] (600/700–450/500)	Argonne V_{18} [92]
0–100	795	1.0–1.7	1.0–3.8	1.0
100–190	411	1.5–1.9	3.5–11.6	1.3
190–290	851	1.9–2.7	4.3–44.4	1.8
0–290	2057	1.5–2.1	2.9–22.3	1.4

have already revealed. For the low-energy scattering and deuteron parameters, see Ref. [34].

5 Few-nucleon forces

The chiral 2NF discussed in the previous section has been applied in microscopic calculations of nuclear structure with, in general, a great deal of success [41, 42, 43, 44, 45, 46, 47, 48, 49, 50, 51, 52, 53, 54, 55]. However, from high-precision studies conducted in the 1990s, it is well-known that certain few-nucleon reactions and nuclear structure issues require 3NFs for their microscopic explanation. Outstanding examples are the A_y puzzle of N-d scattering [99, 100] and the ground state of ^{10}B [101]. As noted before, an important advantage of the EFT approach to nuclear forces is that it creates two- and many-nucleon forces on an equal footing (cf. the overview given in Fig. 1).

For a 3NF, we have $A = 3$ and $C = 1$ and, thus, Eq. (5) implies

$$\nu = 2 + 2L + \sum_i \Delta_i \, . \tag{15}$$

This equation can be used to analyze 3NF contributions order by order. The lowest possible power is obviously $\nu = 2$ (NLO), which is obtained for no loops ($L = 0$) and only leading vertices ($\sum_i \Delta_i = 0$). This 3NF happens to vanish [18, 77, 78]. The first non-vanishing 3NF occurs at NNLO.

The power $\nu = 3$ (NNLO) is obtained when there are no loops ($L = 0$) and $\sum_i \Delta_i = 1$, i.e., $\Delta_i = 1$ for one vertex while $\Delta_i = 0$ for all other vertices. There are three topologies which fulfill this condition, known as the two-pion exchange (2PE), 1PE, and contact graphs [36, 37] (Fig. 3).

The 2PE 3N-potential is given by

$$V^{\rm 3NF}_{\rm 2PE} = \left(\frac{g_A}{2f_\pi} \right)^2 \frac{1}{2} \sum_{i \neq j \neq k} \frac{(\vec\sigma_i \cdot \vec q_i)(\vec\sigma_j \cdot \vec q_j)}{(q_i^2 + m_\pi^2)(q_j^2 + m_\pi^2)} \; F^{ab}_{ijk} \; \tau^a_i \tau^b_j \tag{16}$$

with $\vec q_i \equiv \vec{p_i}' - \vec p_i$, where $\vec p_i$ and $\vec{p_i}'$ are the initial and final momenta of nucleon i, respectively, and

$$F^{ab}_{ijk} = \delta^{ab} \left[- \frac{4c_1 m_\pi^2}{f_\pi^2} + \frac{2c_3}{f_\pi^2} \; \vec q_i \cdot \vec q_j \right] + \frac{c_4}{f_\pi^2} \sum_c \epsilon^{abc} \; \tau^c_k \; \vec\sigma_k \cdot [\vec q_i \times \vec q_j] \, . \tag{17}$$

There are great similarities between this force and earlier derivations of 2PE 3NFs, notably the 50-year old Fujita-Miyazawa [102], the Tucson-Melbourne (TM) [103], and the Brazil [104] forces. This is also the 3NF advocated by Gerry Brown in Refs. [3, 2].

The 1PE contribution is

$$V^{\rm 3NF}_{\rm 1PE} = -D \; \frac{g_A}{8f^2_\pi} \sum_{i \neq j \neq k} \frac{\vec\sigma_j \cdot \vec q_j}{q^2_j + m^2_\pi} (\boldsymbol{\tau}_i \cdot \boldsymbol{\tau}_j)(\vec\sigma_i \cdot \vec q_j) \tag{18}$$

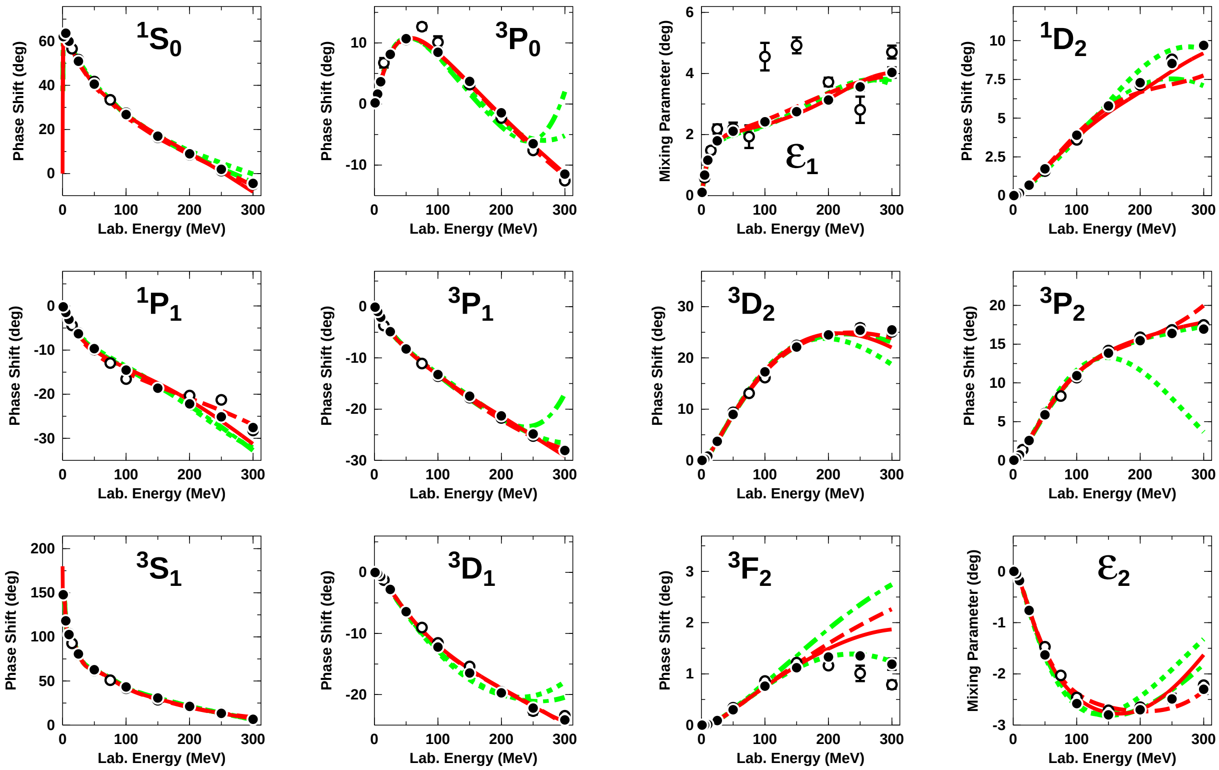

Figure 2: Neutron-proton phase parameters as described by various chiral potentials at N^{3}LO. The (red) solid and the dashed curves are calculated from Idaho N^{3}LO potentials [34] with $\Lambda = 500$ and 600 MeV, respectively; while the (green) dash-dotted and the dotted curves are based upon Juelich N^{3}LO potentials [86] with cutoff combinations 600/700 and 450/500 MeV, respectively. Partial waves with total angular momentum $J \leq 2$ and laboratory energies up to 300 MeV are displayed. The solid dots and open circles are the results from the Nijmegen multi-energy np phase shift analysis [90] and the VPI/GWU single-energy np analysis SM99 [98], respectively.

and the 3N contact potential reads

$$V_{\rm ct}^{\rm 3NF} = E\,\frac{1}{2}\sum_{j\neq k} \boldsymbol{\tau}_j \cdot \boldsymbol{\tau}_k \,. \tag{19}$$

The last two 3NF terms involve the two new parameters D and E, which do not appear in the 2N problem. There are many ways to pin these two parameters down. In Ref. [37], the triton binding energy and the nd doublet scattering length $^2a_{nd}$ were used. One may also choose the binding energies of ^{3}H and ^{4}He [65] or an optimal over-all fit of the properties of light nuclei [66]. Once D and E are fixed, the results for other 3N, 4N, etc. observables are predictions.

The 3NF at NNLO has been applied in calculations of few-nucleon reactions [37, 56, 57, 58, 59, 60, 61, 62, 63, 64], structure of light- and medium-mass nuclei [65, 66, 67, 68], and nuclear and neutron matter [69, 70] with a good deal of success. Yet, the famous 'A_y puzzle' of nucleon-deuteron scattering is not resolved [37, 61]. When only 2NFs are applied, the analyzing power in p-^{3}He scattering is even more underpredicted than in p-d [40, 105]. However, when the NNLO 3NF is added, the p-^{3}He A_y substantially improves (more than in p-d) [64]—but a discrepancy remains. Furthermore, the spectra of light nuclei leave room for improvement [66].

To summarize, the 3NF at NNLO is a remarkable contribution: It represents the leading many-body force within the scheme of ChPT; it includes terms that were advocated by Gerry Brown already some 40 years

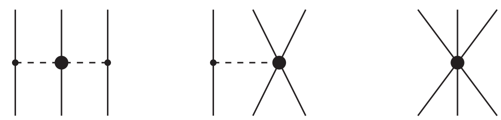

Figure 3: The three-nucleon force at NNLO. From left to right: 2PE, 1PE, and contact diagrams. Notation as in Fig. 1.

ago [3, 2]; and it produces noticeable improvements in few-nucleon reactions and the structure of light nuclei. But unresolved problems remain. Moreover, in the case of the 2NF, we have seen that one has to proceed to N^{3}LO to achieve sufficient accuracy. Therefore, the 3NF at N^{3}LO is needed for at least two reasons: for consistency with the 2NF and to hopefully resolve outstanding problems in microscopic structure and reactions. For further discussion of the 3NF (beyond NNLO), see Ref. [81].

6 Conclusions and Outlook

Forty years after Gerry Brown had stressed repeatedly the outstanding importance of chiral symmetry, we have finally arrived at a derivation of nuclear forces which takes this symmetry consistently into account.

The greatest progress occurred during the past 15 years. Key to this development was the realization that low-energy QCD is equivalent to a chiral effective field theory which allows for a perturbative expansion that has become known as chiral perturbation theory (ChPT). In this framework, two- and many-body forces emerge on an equal footing and the empirical fact that nuclear many-body forces are substantially weaker than the two-nucleon force is explained naturally.

In this chapter, we have shown how the two-nucleon force is derived from ChPT and demonstrated that, at N^{3}LO, the accuracy can be achieved that is necessary and sufficient for reliable microscopic nuclear structure predictions. First calculations applying the N^{3}LO NN potential [34] in the conventional shell model [41, 42, 43], the *ab initio* no-core shell model [44, 45, 46], the coupled cluster formalism [47, 48, 49, 50, 51, 52, 53], and the unitary-model-operator approach [54, 55] have produced promising results.

We also discussed nuclear many-body forces based upon chiral EFT. The 3NF at NNLO has been known for a while [36, 37] and applied in few-nucleon reactions [37, 56, 57, 58, 59, 60, 61, 62, 63, 64], structure of light- and medium-mass nuclei [65, 66, 67, 68], and nuclear and neutron matter [69, 70] with good success; but some open issues remain, which are presently under investigation [81].

We are optimistic that the remaining outstanding problems will be resolved within the next few years, such that, after 80 years of desperate struggle, we may finally claim that the nuclear force problem is essentially under control—last not least, due to a thorough accounting of chiral symmetry.

Acknowledgement

It is our great pleasure to dedicate this chapter to Gerry Brown on the occasion of his 85th birthday. One of us (R.M.) has been a postdoc with Gerry during the years of 1976 and 1977 and stayed in contact with him ever since. R.M. has always been impressed by Gerry's liberating personality and inspiring physics intuition. This work was supported in part by the U.S. Department of Energy under Grant No. DE-FG02-03ER41270 (R.M.), and the Ministerio de Ciencia y Tecnología under Contract No. FPA2007-65748 and the Junta de Castilla y León under Contract Nos. SA-106A07 and GR12 (D.R.E.).

References

[1] G. E. Brown, Comments Nucl. Part. Phys. **4** (1970) 140.

[2] G. E. Brown, in: Meson in Nuclei, Vol. I, edited by M. Rho and D. H. Wilkinson (North-Holland, Amsterdam, 1979) p. 330.

[3] G. E. Brown, A. M. Green, and W J. Gerace, Nucl. Phys. **A115** (1968) 435.

[4] J. Schwinger, Ann. Phys. (N.Y.) **2** (1957) 407.

[5] M. Gell-Mann and M. Levy, Nuovo Cimento **16** (1960) 705.

[6] T. Ericson and W. Weise, *Pions and Nuclei* (Clarendon Press, Oxford, 1988).

[7] S. Weinberg, Phys. Rev. Lett. **18** (1967) 188.

[8] S. Weinberg, Phys. Rev. Lett. **17** (1966) 616.

[9] Y. Tomozawa, Nuovo Cimento A **46** (1966) 707.

[10] S. Weinberg, Phys. Rev. **166** (1968) 1568.

[11] S. Coleman, J. Wess, and B. Zumino, Phys. Rev. **177** (1969) 2239; C. G. Callan, S. Coleman, J. Wess, and B. Zumino, *ibid.* **177** (1969) 2247.

[12] S. Weinberg, Physica **96A** (1979) 327.

[13] S. Weinberg, *Effective Field Theory, Past and Future*, arXiv:0908:1964 [hep-th].

[14] J. Gasser and H. Leutwyler, Ann. Phys. **158** (1984) 142; Nucl. Phys. **B250** (1985) 465.

[15] J. Gasser, M. E. Sainio, and A. Švarc, Nucl. Phys. **B307** (1986) 779.

[16] S. Weinberg, Phys. Lett. B **251** (1990) 288.

[17] S. Weinberg, Nucl. Phys. **B363** (1991) 3.

[18] S. Weinberg, Phys. Lett. B **295** (1992) 114.

[19] C. Ordóñez, L. Ray, and U. van Kolck, Phys. Rev. Lett. **72** (1994) 1982.

[20] C. Ordóñez, L. Ray, and U. van Kolck, Phys. Rev. C **53** (1996) 2086.

[21] N. Kaiser, R. Brockmann, and W. Weise, Nucl. Phys. **A625** (1997) 758.

[22] N. Kaiser, S. Gerstendörfer, and W. Weise, Nucl. Phys. **A637** (1998) 395.

[23] N. Kaiser, Phys. Rev. C **61** (2000) 014003.

[24] N. Kaiser, Phys. Rev. C **62** (2000) 024001.

[25] N. Kaiser, Phys. Rev. C **63** (2001) 044010.

[26] N. Kaiser, Phys. Rev. C **64** (2001) 057001.

[27] N. Kaiser, Phys. Rev. C **65** (2002) 017001.

[28] C. A. da Rocha and M. R. Robilotta, Phys. Rev. C **49** (1994) 1818; **52** (1995) 531; M. R. Robilotta, Nucl. Phys. **A595** (1995) 171; M. R. Robilotta and C. A. da Rocha, Nucl. Phys. **A615** (1997) 391; J.-L. Ballot, C. A. da Rocha, and M. R. Robilotta, Phys. Rev. C **57** (1998) 1574.

[29] R. Higa and M. R. Robilotta, Phys. Rev. C **68** (2003) 024004.

[30] E. Epelbaum, W. Glöckle, and U.-G. Meißner, Nucl. Phys. **A637** (1998) 107.

[31] E. Epelbaum, W. Glöckle, and U.-G. Meißner, Nucl. Phys. **A671** (2000) 295.

[32] D. R. Entem and R. Machleidt, Phys. Lett. B **524** (2002) 93.

[33] D. R. Entem and R. Machleidt, Phys. Rev. C **66** (2002) 014002.

[34] D. R. Entem and R. Machleidt, Phys. Rev. C **68** (2003) 041001.

[35] R. Machleidt and D. R. Entem, J. Phys. G: Nucl. Phys. **31** (2005) S1235.

[36] U. van Kolck, Phys. Rev. C **49** (1994) 2932.

[37] E. Epelbaum *et al.*, Phys. Rev. C **66** (2002) 064001.

[38] S. Ishikawa and M. R. Robilotta, Phys. Rev. C **76** (2007) 014006.

[39] V. Bernard, E. Epelbaum, H. Krebs, and U.-G. Meißner, Phys. Rev. C **77** (2008) 064004.

[40] A. Deltuva and A. C. Fonseca, Phys. Rev. Lett. **98** (2007) 162502; Phys. Rev. C **76**, (2007) 021001; arXiv:1005.1308 [nucl-th].

[41] L. Coraggio *et al.*, Phys. Rev. C **66** (2002) 021303.

[42] L. Coraggio *et al.*, Phys. Rev. C **71** (2005) 014307.

[43] L. Coraggio *et al.*, arXiv:1005.2896 [nucl-th].

[44] P. Navrátil and E. Caurier, *Phys. Rev. C* **69** (2004) 014311.

[45] C. Forssen *et al.*, Phys. Rev. C **71** (2005) 044312.

[46] J.P. Vary *et al.*, Eur. Phys. J. A **25** s01 (2005) 475.

[47] K. Kowalski *et al.*, Phys. Rev. Lett. **92** (2004) 132501.

[48] D.J. Dean and M. Hjorth-Jensen, *Phys. Rev.* C **69** (2004) 054320.

[49] M. Wloch *et al.*, J. Phys. G **31** (2005) S1291; Phys. Rev. Lett. **94** (2005) 21250.

[50] D.J. Dean *et al.*, Nucl. Phys. **752** (2005) 299.

[51] J.R. Gour *et al.*, Phys. Rev. C **74** (2006) 024310.

[52] G. Hagen, T. Papenbrock, D. J. Dean, and M. Hjorth-Jensen, Phys. Rev. Lett. **101** (2008) 092502.

[53] G. Hagen, T. Papenbrock, D. J. Dean, and M. Hjorth-Jensen, Phys. Rev. C **82**, 034330 (2010).

[54] S. Fujii, R. Okamoto, and K. Suzuki, Phys. Rev. C **69** (2004) 034328.

[55] S. Fujii, R. Okamoto, and K. Suzuki, Phys. Rev. Lett. **103** (2009) 182501.

[56] K. Ermisch *et al.*, Phys. Rev. C **71** (2005) 064004.

[57] S. Kistryn *et al.*, Phys. Rev. C **72** (2005) 044006.

[58] H. Witala, J. Golak, R. Skibinski, W. Glöckle, A. Nogga, E. Epelbaum, H. Kamada, A. Kievsky, and M. Viviani, Phys. Rev. C **73** (2006) 044004.

[59] J. Ley *et al.*, Phys. Rev. C **73** (2006) 064001.

[60] E. Stephan *et al.*, Phys. Rev. C **76** (2007) 057001.

[61] N. Kalantar-Nayestanaki and E. Epelbaum, *The three-nucleon system as a laboratory for nuclear physics: the need for 3N forces*, Nucl. Phys. News **17** (2007) 22, arXiv:nucl-th/0703089, and references therein.

[62] L. C. Marcucci, A. Kievsky, L. Girlanda, S. Rosati, and M. Viviani, Phys. Rev. C **80** (2009) 034003.

[63] A. Kievsky, M. Viviani, L. Girlanda, and L. E. Marcucci, Phys. Rev. C **81** (2010) 044003.

[64] M. Viviani, L. Giarlanda, A. Kievsky, L. E. Marcucci, and S. Rosati, arXiv:1004.1306 [nucl-th].

[65] A. Nogga, P. Navratil, B. R. Barrett, and J. P. Vary, Phys. Rev. C **73** (2006) 064002.

[66] P. Navratil, V. G. Gueorguiev, J. P. Vary, W. E. Ormand, and A. Nogga, Phys. Rev. Lett. **99** (2007) 042501.

[67] G. Hagen *et al*, Phys. Rev. C **76** (2007) 034302.

[68] T. Otsuka, T. Susuki, J. D. Holt, A. Schwenk, and Y. Akaishi, Phys. Rev. Lett. **105** (2010) 03250.

[69] S. K. Bogner *et al.*, Nucl. Phys. **A763** (2005) 59; S. K. Bogner *et al.*, *Nuclear matter from chiral low-momentum interactions*, arXiv:0903.3366 [nucl-th].

[70] K. Hebeler and A. Schwenk, Phys. Rev. C **82**, 014314 (2010).

[71] S. R. Beane, P. F. Bedaque, K. Orginos, and M. J. Savage, Phys. Rev. Lett. **97** (2006) 012001.

[72] N Ishii, S. Aoki, and T. Hatsuda, Phys. Rev. Lett. **99** (2007) 022001.

[73] J. Goldstone, Nuovo Cim. **19** (1961) 154.

[74] J. Goldstone, A. Salam, and S. Weinberg, Phys. Rev. **127** (1962) 965.

[75] R. Machleidt, K. Holinde, and Ch. Elster, Phys. Rep. **149** (1987) 1.

[76] M. Lacombe, B. Loiseau, J. M. Richard, R. Vinh Mau, J. Côté, P. Pires, and R. de Tourreil, Phys. Rev. C **21** (1980) 861.

[77] S. N. Yang and W. Glöckle, Phys. Rev. C **33** (1986) 1774.

[78] S. A. Coon and J. L. Friar, Phys. Rev. C **34** (1986) 1060.

[79] R. Machleidt, Adv. Nucl. Phys. **19** (1989) 189.

[80] D. B. Kaplan, M. J. Savage, and M. B. Wise, Nucl. Phys. **B478** (1996) 629; Phys. Lett. B **424** (1998) 390; Nucl. Phys. **B534** (1998) 329.

[81] R. Machleidt and D. R. Entem, J. Phys. G: Nucl. Part. Phys. **37**, 064041 (2010).

[82] A. Nogga, R. G. E. Timmermans, and U. van Kolck, Phys. Rev. C **72** (2005) 054006.

[83] M. P. Valderrama, Phys. Rev. C **83**, 024003 (2011).

[84] R. Machleidt, P. Liu, D. R. Entem, and E. Ruiz Arriola, Phys. Rev. C **81** (2010) 024001.

[85] G. P. Lepage, *How to Renormalize the Schrödinger Equation*, nucl-th/9706029.

[86] E. Epelbaum, W. Glöckle, and U.-G. Meißner, Nucl. Phys. A747 (2005) 362.

[87] The 1999 NN data base is defined in Ref. [88].

[88] R. Machleidt, Phys. Rev. C **63** (2001) 024001.

[89] E. Epelbaum, W. Glöckle, and U.-G. Meißner, Eur. Phys. J. **A19** (2004) 401.

[90] V. G. J. Stoks, R. A. M. Klomp, M. C. M. Rentmeester, and J. J. de Swart, Phys. Rev. C **48** (1993) 792.

[91] V. G. J. Stoks, R. A. M. Klomp, C. P. F. Terheggen, and J. J. de Swart, Phys. Rev. C **49** (1994) 2950.

[92] R. B. Wiringa, V. G. J. Stoks, and R. Schiavilla, Phys. Rev. C **51** (1995) 38.

[93] R. Machleidt, F. Sammarruca, and Y. Song, Phys. Rev. C **53** (1996) 1483.

[94] M. Walzl *et al.*, Nucl. Phys. **A693**, 663 (2001).

[95] U. van Kolck *et al.*, Phys. Rev. Lett. **80** (1998) 4386.

[96] P. Büttiker *et al.*, Nucl. Phys. **A668**, 97 (2000).

[97] N. Fettes *et al.*, Nucl. Phys. **A640**, 199 (1998).

[98] R. A. Arndt, I. I. Strakovsky, and R. L. Workman, SAID, Scattering Analysis Interactive Dial-in computer facility, George Washington University (formerly Virginia Polytechnic Institute), solution SM99 (Summer 1999); for more information see, e. g., R. A. Arndt, I. I. Strakovsky, and R. L. Workman, Phys. Rev. C **50** (1994) 2731.

[99] W. Glöckle *et al.*, Phys. Rep. **274** (1996) 107.

[100] D. R. Entem, R. Machleidt, and H. Witala, Phys. Rev. C **65** (2002) 064005, and references to earlier work therein.

[101] E. Caurier *et al.*, Phys. Rev. C **66** (2002) 024314.

[102] J.-I. Fujita and H. Miyazawa, Prog. Theor. Phys. **17** (1957) 360.

[103] S. A. Coon, M. D. Scadron, P. C. McNamee, B. R. Barrett, D. W. E. Blatt. and B. H. J. McKeller, Nucl. Phys. **A317** (1979) 242.

[104] H. T. Coelho, T. K. Das, and M. R. Robilotta, Phys. Rev. C **28** (1983) 1812; M. R. Robilotta and H. T. Coelho, Nucl. Phys. **A460** (1986) 645.

[105] B. M. Fisher *et al.*, Phys. Rev. C **74** (2006) 034001.